

Jinzhe Gong, Aaron C. Zecchin, Martin F. Lambert, and Angus R. Simpson

Determination of the creep function of viscoelastic pipelines using system resonant frequencies with hydraulic transient analysis

Journal of Hydraulic Engineering, 2016; Online Publ:04016023

Published at:

<http://ascelibrary.org/doi/10.1061/%28ASCE%29HY.1943-7900.0001149>

PERMISSIONS

<http://ascelibrary.org/page/informationforasceauthorsreusingyourownmaterial>

Draft Manuscript

Authors may post the final draft of their work on open, unrestricted Internet sites or deposit it in an institutional repository when the draft contains a link to the bibliographic record of the published version in the [ASCE Library](#) or [Civil Engineering Database](#). "Final draft" means the version submitted to ASCE after peer review and prior to copyediting or other ASCE production activities; it does not include the copyedited version, the page proof, or a PDF of the published version.

14 June, 2016

<http://hdl.handle.net/2440/99583>

1 **Determination of the creep function of viscoelastic**
2 **pipelines using system resonant frequencies with**
3 **hydraulic transient analysis**

4

5 Jinzhe Gong¹, Aaron C. Zecchin², Martin F. Lambert³ and Angus R. Simpson⁴

6

7 ¹Research Associate; School of Civil, Environmental and Mining Engineering, University
8 of Adelaide, SA 5005, Australia; Email: jinzhe.gong@adelaide.edu.au

9 ²Senior Lecturer; School of Civil, Environmental and Mining Engineering, University of
10 Adelaide, SA 5005, Australia; Email: aaron.zecchin@adelaide.edu.au

11 ³Professor; M.ASCE; School of Civil, Environmental and Mining Engineering, University
12 of Adelaide, SA 5005, Australia; Email: martin.lambert@adelaide.edu.au

13 ⁴Professor; M.ASCE; School of Civil, Environmental and Mining Engineering, University
14 of Adelaide, SA 5005, Australia; Email: angus.simpson@adelaide.edu.au

15

16 **Abstract**

17 The determination of the creep (compliance) function of viscoelastic pipelines is essential
18 for modelling their hydraulic behavior and accurately predicting pressure responses under
19 transient events. This paper proposes a novel frequency-domain technique for the
20 determination of the creep function of viscoelastic pipelines using hydraulic transients. A
21 viscoelastic pipeline system, when compared with a frictionless elastic pipeline under the
22 same system configuration, has non-uniformly shifted resonant frequencies. Analytical

23 analysis shows that the shift in the resonant frequencies of a viscoelastic pipeline system is
24 related to both the pipe wall viscoelastic compliance effects and the unsteady wall shear
25 stress effects. A technique is developed to determine the elastic wave speed and the
26 viscoelastic creep compliances based on the shifted system resonant frequencies. To
27 improve the accuracy of the calibration for the viscoelastic parameters, an approach is
28 proposed to correct the shifting in the resonant frequencies induced by the unsteady friction
29 before the calibration. Numerical simulations conducted on a high-density polyethylene
30 (HDPE) pipeline verify that the elastic wave speed and viscoelastic compliance can be
31 determined with relatively high accuracy.

32 *Keywords:* creep function; fluid transient; polymer; resonance; viscoelasticity; water
33 hammer.

34 **Introduction**

35 Viscoelastic pipelines, such as polyvinyl chloride (PVC) and high-density polyethylene
36 (HDPE) pipelines, have been increasingly used throughout the world for potable water
37 distribution, sewage effluent transport and agriculture irrigation. Experimental studies
38 (Güney 1983; Covas et al. 2004; Ramos et al. 2004; Brunone and Berni 2010; Meniconi et
39 al. 2012; Pezzinga et al. 2014) showed that transient pressure waves experienced greater
40 attenuation and dispersion in viscoelastic pipelines when compared with elastic pipelines
41 (e.g. metallic pipes). However, in some cases, the use of viscoelastic pipelines increases
42 the maximum transient pressure (Pezzinga and Scandura 1995; Ramos et al. 2004). In the
43 frequency domain, viscoelasticity introduces non-uniform (frequency-dependent) shifting

44 of the resonant frequencies of a pipeline system and non-uniform resonant responses (Suo
45 and Wylie 1990; Lee et al. 2013). Detailed understanding of the hydraulic characteristics
46 of viscoelastic pipelines is critical for accurate prediction of the pressure responses of a
47 pipeline system during transient events, better system design and safe operation.

48 A number of studies, both in the time and the frequency domain, have been conducted and
49 reported in the literature on the development of a mathematical model to describe the
50 hydraulic transient response of viscoelastic pipelines. For an applied pressure load within
51 a pipe (as experienced during a water hammer event), the effect of viscoelasticity is
52 characterized by an instantaneous elastic strain, followed by a gradual retarded strain
53 (Covas et al. 2004; Shaw and MacKnight 2005). In the time domain, the method of
54 characteristics (MOC) (Wylie and Streeter 1993; Chaudhry 2014) was used and an
55 additional viscoelastic term was added into the classic continuity equation to describe the
56 retarded wall deformation (Gally et al. 1979; Rieutord and Blanchard 1979; Güney 1983;
57 Pezzinga and Scandura 1995; Ramos et al. 2004; Covas et al. 2005; Soares et al. 2008;
58 Meniconi et al. 2012; Meniconi et al. 2014). Within all this work, a linear viscoelastic
59 mechanical model, the generalized Kelvin-Voigt (K-V) model (Shaw and MacKnight 2005)
60 that includes an elastic element and one or more viscoelastic elements, was used to describe
61 the retarded wall deformation by mathematically describing the creep function of a
62 viscoelastic pipeline. The creep function, which is also known as compliance function, is a
63 description of the time variation of strain for a constant stress, and related to the molecular
64 structure of the material, temperature and stress-time history (Covas et al. 2004). In
65 Brunone et al. (2000) it is shown that very large (not physically reasonable) decay

66 coefficients of the friction formula (Brunone et al. 1995) should be used to simulate
67 transients in viscoelastic pipes when viscoelasticity is not taken into account.

68 In the frequency domain, most previous studies of fluid transient simulation in viscoelastic
69 pipelines used a frequency-dependent wave speed to describe the pipeline viscoelasticity,
70 and the modulus of elasticity of a viscoelastic pipeline was represented by the inverse of
71 the creep function (both in the frequency domain) (Meißner and Frank 1977; Rieutord 1982;
72 Franke and Seyler 1983; Suo and Wylie 1990). A different approach was taken by Duan et
73 al. (2012), which derived the transfer matrix of a viscoelastic pipeline, with and without a
74 leak, using the time-domain modified continuity equation and a one-element K-V model.
75 However, the frequency-dependent effects on the size of the resonant responses were not
76 observed in their numerical simulations, i.e. the resonant responses of the intact viscoelastic
77 pipe that was considered showed an almost uniform amplitude.

78 Research on the transient behavior of viscoelastic pipelines has also been extended to
79 numerical stability analysis of the MOC-based simulation with K-V model (Zecchin et al.
80 2008), viscoelastic pipelines with unsteady friction (Covas et al. 2005; Duan et al. 2010a;
81 Duan et al. 2010b), cavitation (Keramat et al. 2010), time-dependent Poisson's ratio
82 (Keramat et al. 2013), fluid structure interaction (Keramat et al. 2012), the presence of
83 leaks (Duan et al. 2012; Ferrante et al. 2013; Lazhar et al. 2013) and blockages (Meniconi
84 et al. 2012; Meniconi et al. 2013; Meniconi et al. 2014), and in networks (Zecchin et al.
85 2012).

86 With the interest of research on viscoelastic pipelines (in particular, pressurized polymeric
87 water pipelines) gradually increasing in more complex scenarios and experimental studies,
88 a critical issue is the accurate evaluation of the creep function, which is the key for accurate
89 prediction of the mechanical behavior and transient response in real viscoelastic pipelines.
90 The creep function of a viscoelastic pipeline can be evaluated by mechanical testing (Zhang
91 and Moore 1997; Covas et al. 2004). However, experiments by Covas et al. (2004) showed
92 that mechanical testing of small samples of the pipe wall material only provided an estimate
93 of the actual mechanical behavior of the pipe system, which depends on not only the
94 molecular structure of the material and temperature but also the pipe axial and
95 circumferential constraints and stress-time history of the pipe system. An alternative
96 approach is to calibrate the mechanical behavior of a pipeline system by hydraulic transient
97 tests. Pezzinga and Scandura (1995) used a one-element K-V model to study a short
98 additional HDPE pipeline connected to a relatively long steel pipeline system. The elastic
99 modulus of elasticity (which corresponds to the elastic component of the pipe's
100 circumferential expansion and manifested by the elastic wave speed) of the HDPE pipe
101 was determined from the oscillation periods of the transient pressure wave, while the
102 viscoelastic parameters were determined by trial-and-error. However, the accuracy of the
103 calibration of the elastic modulus of elasticity (or the elastic wave speed) is hard to assure
104 because the oscillation period is not constant over time in viscoelastic pipes due to wave
105 dispersion. Covas et al. (2004) used the inverse transient analysis (ITA) (Liggett and Chen
106 1994) to calibrate the viscoelastic parameters of a HDPE pipeline by optimizing the
107 parameters in a multi-element K-V model in order to minimizing the difference between
108 the simulated and observed pressure traces. Unsteady friction was considered in the

109 forward modeling to account for the friction-induced damping. However, the elastic wave
110 speed (or the elastic creep) was not calibrated by ITA due to the non-uniqueness of the
111 solutions. It was estimated using the traveling time of the incident wave between two
112 pressure transducers, but the measured wave speed varied with the location of the
113 transducer pairs due to wave dispersion. The ITA approach was adapted in several later
114 studies (Soares et al. 2008; Duan et al. 2010a; Meniconi et al. 2012; Pezzinga 2014).
115 Keramat and Haghghi (2014) developed a ‘viscoelastic Joukowsky formula’ to describe
116 the head response in viscoelastic pipelines induced by a valve closure. Unsteady friction
117 was neglected in the formula. A curve-fitting procedure, which is much more
118 computational efficient than the ITA, was used to calibrate the mechanical parameters by
119 matching the numerical head response with the measurements in the first half water
120 hammer cycle. However, the elastic modulus of elasticity (or the elastic wave speed) was
121 not calibrated but pre-assigned in the case studies reported in Keramat and Haghghi (2014),
122 and the calibrated viscoelastic compliances were significantly different (20% or more)
123 from the values used in the original numerical model. Overall, all the previous hydraulic
124 transient-based studies on the calibration of the creep function of viscoelastic water
125 pipelines were limited to time-domain analysis. The parameter calibration, even for the
126 elastic modulus of elasticity (or the elastic wave speed) alone, is very challenging due to
127 the significant wave dispersion and the fact that unsteady friction also introduces wave
128 attenuation and dispersion.

129 The current research proposes a new technique for calibrating the creep function of
130 viscoelastic pipelines using hydraulic transients but with frequency-domain analysis. The
131 proposed technique only uses information about the resonant frequencies, which is not

132 subject to discrete faults (such as leaks) in pipelines. The analysis of the transfer matrix of
133 a viscoelastic pipeline derived using a generalized multi-element K-V model shows that
134 the use of an additional retarded strain term in the continuity equation and the use of a
135 frequency-dependent wave speed (or frequency-dependent modulus of elasticity) to model
136 the pipeline viscoelastic behavior are equivalent. It is also found that both the
137 viscoelasticity and the unsteady friction introduce frequency-dependent reduction and
138 shifting to the resonant response peaks of a pipeline system. Based on the analytical
139 relationship between the resonant frequencies and the pipeline viscoelastic and friction-
140 related parameters, a technique is developed to determine the elastic wave speed and the
141 viscoelastic compliances from the resonant frequencies. The technique is complemented
142 by an approach to correct the shifting in the resonant frequencies induced by the unsteady
143 friction before the calibration of the viscoelastic parameters. Numerical case studies are
144 conducted on an HDPE pipeline without and with unsteady friction. The results show that
145 the new technique is computationally efficient and can yield accurate evaluation of the
146 elastic wave speed and satisfactory accuracy for the viscoelastic compliances. Challenges
147 for future applications in field pipelines are also identified and discussed in the end of the
148 paper.

149 **Time-domain Governing Equations for Viscoelastic** 150 **Pipelines**

151 This section is a brief review of the time-domain governing equations for viscoelastic
152 pipelines. The one-dimensional (1-D) momentum equation for transient flow in pressurized
153 pipelines is given as (Wylie and Streeter 1993; Chaudhry 2014)

$$\frac{1}{gA} \frac{\partial Q}{\partial t} + \frac{\partial H}{\partial x} + h_f = 0 \quad (1)$$

154 where g is gravitational acceleration, A is the cross-sectional area of a pipeline, Q is the
 155 flow rate, H is the piezometric head, t is time, x is distance along the pipeline, and h_f is
 156 the head loss per unit length due to friction. The head loss can be regarded as a summation
 157 of a steady-state component and an unsteady-state component (Zielke 1968). The steady-
 158 state component is well defined for both laminar and turbulent flow (Wylie and Streeter
 159 1993; Chaudhry 2014). Several unsteady head loss formulas are reported in the literature
 160 (Zielke 1968; Vardy et al. 1993; Brunone et al. 1995; Vítkovský 2006).

161 The one-dimensional continuity equation with a retarded strain term for viscoelastic
 162 pipelines is given as (Gally et al. 1979; Pezzinga and Scandura 1995; Covas et al. 2005)

$$\frac{gA}{a_e^2} \frac{\partial H}{\partial t} + \frac{\partial Q}{\partial x} + 2A \frac{\partial \varepsilon_r}{\partial t} = 0 \quad (2)$$

163 where a_e is the elastic wave speed and ε_r is the retarded strain. a_e is related to the elastic
 164 modulus of elasticity E_0 by the classic wave speed formula (Wylie and Streeter 1993;
 165 Chaudhry 2014).

166 The generalized Kelvin-Voigt (K-V) model has been commonly used to describe the
 167 mechanical behavior (creep function) of a viscoelastic material (Shaw and MacKnight
 168 2005). The model, as illustrated in Figure 1, includes one elastic element and N

169 viscoelastic elements in series connection. The elastic element is represented by a single
170 spring with a modulus of elasticity E_0 (which is referred as the elastic modulus of
171 elasticity), and a viscoelastic element consists of a dashpot with a viscosity η_k and a spring
172 with a modulus of elasticity E_k in parallel connection.

173 Using the K-V model, the creep function is described by

$$J(t) = J_0 + \sum_{k=1}^N J_k (1 - e^{-t/\tau_k}) \quad (3)$$

174 where J_0 equals $1/E_0$ and it is termed as the elastic creep in some literature, J_k equals
175 $1/E_k$ and it is the compliance of the spring of the k th K-V element, τ_k equals η_k / E_k and
176 it is the retardation time of the dashpot of the k th K-V element. Note that the K-V model
177 is a phenomenological model without physical interpretation (Weinerowska-Bords 2006,
178 2007), as a result, different combinations of the number of K-V elements and the values of
179 J_0 , J_k and τ_k may yield very similar creep curves (Covas et al. 2005; Keramat and
180 Haghghi 2014). To reduce the possibility of non-uniqueness in solutions, a recent practice
181 in research is to assume the number of K-V elements and assign constant values to τ_k , then
182 determine the values of J_0 and J_k (Covas et al. 2005; Keramat and Haghghi 2014;
183 Pezzinga 2014). This strategy is also used in the current research.

184 Frequency-domain Governing Equations for Viscoelastic 185 Pipelines

186 *Transfer matrix for a viscoelastic pipeline*

187 The transfer function of a viscoelastic pipeline can be derived using the concept of steady-
188 oscillatory flow, where every transient signal is described as a perturbation about a mean
189 state (Wylie and Streeter 1993; Chaudhry 2014). Using Eqs. (1) and (2) and following the
190 derivation presented in Duan et al. (2012) but using a generalized multiple element K-V
191 model [Eq. (3)], the transfer matrix for a viscoelastic pipeline can be written as

$$\begin{Bmatrix} q \\ h \end{Bmatrix}^{n+1} = \begin{bmatrix} \cosh(\mu L) & -\frac{1}{Z} \sinh(\mu L) \\ -Z \sinh(\mu L) & \cosh(\mu L) \end{bmatrix} \begin{Bmatrix} q \\ h \end{Bmatrix}^n \quad (4)$$

192 where q and h are the complex flow and head oscillation in the frequency domain, L is
193 the total length of the pipe, and the propagation operator μ and the characteristic
194 impedance Z are given by

$$\mu = \frac{i\omega}{a_e} T_{VE} T_F \quad (5)$$

$$Z = \frac{a_e T_F}{gA T_{VE}} \quad (6)$$

195 in which ω is the angular frequency, T_{VE} and T_F represent the terms contributed by
 196 viscoelasticity and friction, respectively, and are given as

$$T_{VE} = \sqrt{1 + a_e^2 \frac{\alpha D \rho}{e} \sum_{k=1}^N \frac{J_k}{i\omega\tau_k + 1}} \quad (7)$$

$$T_F = \sqrt{1 + \frac{gA}{i\omega} R} \quad (8)$$

197 where α is the pipeline restraint factor, D is the pipeline internal diameter, ρ is the
 198 density of fluid, e is pipe wall thickness, R is the resistance per unit length. More details
 199 for the derivation of Eqs. (5) to (8) can be found in Gong et al. (2015b).

200 R can be described by a summation of the steady friction part R_s and the unsteady friction
 201 part R_{us} , i.e. $R = R_s + R_{us}$, where $R_s = fQ_0 / (gDA^2)$ is the linearized steady-state
 202 resistance term for smooth-pipe turbulent flow and f is the Darcy-Weisbach friction
 203 factor. The expression of R_{us} presented in Vítkovský et al. (2003) is used in this research.
 204 The R_{us} term was derived based on the Zielke (1968) unsteady friction model and the
 205 Vardy and Brown (1995; 1996) weighting function for smooth-pipe turbulent flow.

206 ***Modelling pipe viscoelasticity by retarded strain versus by***
 207 ***complex wave speed***

208 A further analysis of Eqs. (5) and (6) shows that, the existing two approaches of modeling
 209 pipe wall viscoelastic effects on transient pressure waves as reported in literature [i.e. the

210 use of an additional term ($2A\partial\varepsilon_r/\partial t$) to represent the retarded strain (Gally et al. 1979;
 211 Rieutord and Blanchard 1979; Güney 1983; Pezzinga and Scandura 1995; Ramos et al.
 212 2004; Covas et al. 2005; Soares et al. 2008; Meniconi et al. 2012; Meniconi et al. 2014)
 213 and the use of a frequency-dependent and complex wave speed (Rieutord 1982; Suo and
 214 Wylie 1990)], are equivalent, despite apparent differences in their representations. In
 215 Rieutord (1982) and Suo and Wylie (1990), the pipeline viscoelasticity was modeled by
 216 only considering a frequency-dependent and complex modulus of elasticity $E(i\omega)$, which
 217 is defined as $1/J(i\omega)$ and $J(i\omega)$ is the frequency domain representation of the creep
 218 function shown in Eq.(3). The use of $E(i\omega)$ resulted in a frequency-dependent and
 219 complex wave speed a^* as given by the classic wave speed formula for elastic pipes
 220 (Rieutord 1982; Suo and Wylie 1990)

$$a^* = \sqrt{\frac{K/\rho}{1 + \alpha(K/E(i\omega))(D/e)}} \quad (9)$$

221 To model the pipe wall viscoelastic effects for transient pressure waves, instead of the use
 222 of an additional term for the retarded strain, a^* was used in the classic continuity equation
 223 for elastic pipes to replace the elastic wave speed (Rieutord 1982; Suo and Wylie 1990).

224 Considering the governing equations [Eqs. (5) and (6)] resulted from the use of an
 225 additional term for the retarded strain in the continuity equation, the ratio of a_e to T_{AE} can
 226 be regarded as a single parameter a_c . The use of a_c also transforms the format of the

227 propagation operator μ [Eq. (5)] and the characteristic impedance Z [Eq. (6)] to their
 228 counterparts for elastic pipes. a_c in its full expression is written as

$$a_c = \frac{a_e}{\sqrt{1 + a_e^2 \frac{\alpha D \rho}{e} \sum_{k=1}^N \frac{J_k}{i\omega\tau_k + 1}}} \quad (10)$$

229 where the elastic wave speed a_e is given by the classical wave speed formula for elastic
 230 pipes [same format as Eq. (9) but with a constant modulus of elasticity E_0]. Further
 231 mathematical arrangements show that a_c as given in Eq. (10) is indeed the same as the
 232 frequency-dependent and complex wave speed a^* as derived from the complex modulus
 233 of elasticity in Eq. (9). This finding indicates that the use of an additional viscoelastic term
 234 to represent the retarded strain is equivalent to the use of a frequency-dependent and
 235 complex wave speed (or modulus of elasticity) in the continuity equation. In other words,
 236 the mechanical characteristics of viscoelastic pipelines (an instantaneous elastic strain
 237 followed by a retarded strain) lead to a frequency-dependent wave speed. As a result, the
 238 pipeline viscoelasticity is more suitable to be analyzed in the frequency domain, where the
 239 pipe response to loadings with various frequencies can be studied independently.

240 ***Frequency response function of a viscoelastic pipeline***

241 The frequency response function (FRF) of a viscoelastic pipeline can be derived using the
 242 pipeline transfer matrix in Eq. (4) with boundary conditions. In this research, a reservoir-
 243 pipeline-high loss valve system is considered for the analytical derivation, and the special

244 case of a reservoir-pipeline-closed valve configuration is also studied in the numerical
 245 analysis. A side-discharge valve located just upstream of the high loss inline valve acts as
 246 the transient generator. Either discrete signals, such as a pulse (Lee et al. 2006), or
 247 continuous signals, such as pseudo random binary signals (Gong et al. 2015a), can be used
 248 as the excitation. In this research, a discrete discharge perturbation is considered as the
 249 input signal to the system, which can be realized by a fast successive opening and closing
 250 valve maneuver. The discharge perturbation then introduces head perturbations in the
 251 pipeline system, which are considered as the output of the system. Note that under linear
 252 system theory, for a system with a specific configuration, the system response function is
 253 independent of the format of the input excitation (or the type of valve maneuver provided
 254 the input is independent of the output). A discharge perturbation can be described by (Lee
 255 et al. 2006)

$$\begin{Bmatrix} q \\ h \end{Bmatrix}^{n+1} = \begin{bmatrix} 1 & 0 \\ 0 & 1 \end{bmatrix} \begin{Bmatrix} q \\ h \end{Bmatrix}^n + \begin{bmatrix} \Delta q \\ 0 \end{bmatrix} \quad (11)$$

256 where Δq is the discharge perturbation induced by the valve.

257 Applying the transfer matrix method (Wylie and Streeter 1993; Chaudhry 2014) and the
 258 procedure used in elastic pipelines (Lee et al. 2006; Duan et al. 2012; Gong et al. 2013),
 259 the normalized complex head oscillation (frequency response function) at the downstream
 260 end of the pipeline (upstream side of the high loss valve) can be derived as

$$h^* = \frac{Z \tanh(\mu L)}{1 + [Z \tanh(\mu L)/Z_v]} \quad (12)$$

261 where h^* is the complex head oscillation normalized by the active input Δq , Z_v is the
 262 impedance of the high loss inline valve, and L is the length of the pipeline. Note that Eq.
 263 (12) is an expression of the normalized head response for either elastic or viscoelastic
 264 pipeline in a reservoir-pipeline-high loss valve system, and it is independent from the
 265 properties of the excitation. When the T_{vE} and T_F terms as defined in Eqs. (7) and (8) are
 266 used in μ and Z , the head response is for a viscoelastic pipeline with unsteady friction.
 267 The plot of the absolute value of Eq. (12) versus frequency is known as the Frequency
 268 Response Diagram (FRD) for the pipeline system, and the peaks (i.e. maxima) in the FRD
 269 are resonant responses of the system corresponding to the resonant frequencies (i.e. peak
 270 frequencies).

271 **Determination of the Creep Function using Resonant** 272 **Frequencies**

273 This section describes the proposed technique for calibrating the viscoelastic parameters in
 274 the creep function for viscoelastic pipelines. The technique is developed based on the
 275 analytical relationship between the resonant frequencies of a viscoelastic pipeline and the
 276 pipeline viscoelastic and friction-related parameters. As unsteady friction also contributes
 277 to the shifting of the resonant frequencies, an approach is developed to correct the effects
 278 induced by the unsteady friction before the calibration of the viscoelastic parameters.

279 **Approach**

280 For an intact viscoelastic pipeline in a reservoir-pipeline-high loss valve system, the
281 resonant responses are obtained when the absolute value of Eq. (12) reaches its maxima,
282 where the corresponding frequencies are the resonant frequencies. When the inline valve
283 is a high loss valve or fully closed so that the value of Z_v is much greater than the value
284 of $|Z \tanh(\mu L)|$, Eq. (12) can be simplified as

$$h^* = Z \tanh(\mu L) \quad (13)$$

285 with negligible impacts on the resonant frequencies.

286 The characteristic impedance Z is a frequency-dependent function and related to the
287 viscoelastic and friction terms, but its values are unknown when the viscoelastic parameters
288 are unknown. Numerical simulations show that Z is a monotonic function of frequency
289 (presented later in Figure 7). To simplify the analysis, an assumption is made that the
290 influence of Z on the maxima or minima of Eq. (13) can be neglected (implications are
291 further discussed in the later section *Discussions*). In other words, it is assumed that the
292 measured resonant frequencies [which are actually the peak frequencies of the function in
293 Eq. (12)] are the frequencies where the function $|\tanh(\mu L)|$ reaches its maxima.

294 From the mathematic properties of hyperbolic functions (Kreyszig et al. 2011), the
295 hyperbolic tangent is periodic with respect to the imaginary component and the period is
296 πi , where i represents the imaginary unit. For a complex hyperbolic tangent function

297 $\tanh(x + yi)$ with a specific real part x , the maxima of the absolute value of the function
 298 (i.e. $|\tanh(x + yi)|$) are obtained when the imaginary part y is an odd multiple of $\pi / 2$. A
 299 3D mesh plot of function $|\tanh(x + yi)|$ is given in Figure 2.

300 The real and the imaginary parts of the propagation operator μ are monotonic functions
 301 of frequency. The results of $|\tanh(\mu L)|$ for the practical HDPE pipeline considered in the
 302 *Case Studies* section are shown as the thick line in Figure 2, which can be considered as a
 303 curved slice of the 3D mesh. It can be seen that the maxima of the function $|\tanh(\mu L)|$ are
 304 achieved at specific frequencies where the imaginary part of the variable are odd multiples
 305 of $\pi / 2$, i.e.

$$\text{Im}[\mu(\omega_m)L] = (2m-1)\frac{\pi}{2} \quad (14)$$

306 where $\text{Im}[\]$ signifies the imaginary part of the complex number in the brackets, ω_m
 307 represent the resonant angular frequencies, m is an integer ($m = 1, 2, 3 \dots$) and represents
 308 the ordinal number of the resonant peaks.

309 Substituting Eq. (5) into Eq. (14) and applying mathematical manipulation yields

$$\omega_m = (2m-1)\frac{a_e\pi}{\text{Re}[T_{VE}(\omega_m)T_F(\omega_m)]2L} \quad (15)$$

310 where $\text{Re}[\]$ signifies the real part of the complex number in the brackets. Eq. (15) shows
311 that the resonant frequencies of a viscoelastic pipeline is a function of the elastic wave
312 speed a_e , the viscoelastic term T_{VE} , the friction term T_F and the length of pipe L . As a
313 result, it is possible to calibrate the value of a_e (which is related to the elastic creep J_0)
314 and the viscoelastic parameters in T_{VE} and the friction-related parameters in T_F by using
315 known resonant (angular) frequencies ω_m , which can be read from a measured FRD as the
316 peak frequencies. By this approach, the calibration of the viscoelastic parameters in T_{VE} is
317 transferred to a problem of solving a set of nonlinear equations, defined by Eq. (15), and
318 the number of equations to be used depends on the number of unknown parameters to
319 calibrate.

320 ***Steps for implementation***

321 The effects of viscoelasticity and friction on the resonant frequencies are coupled as the
322 product of T_{VE} and T_F , which means the solutions may be non-unique if both T_{VE} and T_F
323 are open to calibration. Previous research on elastic pipelines (Lee et al. 2006; Sattar and
324 Chaudhry 2008) concluded that steady friction does not change the resonant frequencies,
325 while the influence of unsteady friction on the resonant frequencies is very limited.
326 Numerical simulations conducted in this research (as shown later in the *Case Studies*
327 section) confirm those findings. However, the current research also discovers that, although
328 neglecting the effects of unsteady friction in a viscoelastic pipeline does not impose much
329 impact on the calibration of the elastic wave speed, it can have a significant impact on the
330 calibration of the viscoelastic compliances, especially for the high order K-V elements. The

331 explanation is that the higher the order an element is in the K-V model, the less influence
332 it has to the hydraulic behavior of the pipeline system. This means the elastic modulus of
333 elasticity, or the elastic wave speed, is the dominant factor and has the greatest influence
334 on the resonant frequencies, while the influence of the viscoelastic compliances decreases
335 with the increase in element order. It is also evident from the definition of the creep function
336 in Eq. (3), where the relative variation in $J(t)$ is less sensitive to the relative variation in
337 the value of higher order J_k . From the perspective of parameter calibration using measured
338 resonant frequencies, the calibration of the elastic compliance is the least sensitive to errors
339 in the measured resonant frequencies, while the sensitivity to error increases with the
340 increase in the order of K-V elements. In other words, it is more difficult to accurately
341 calibrate higher order K-V elements, because a relatively small error in the measured
342 resonant frequencies would have to be explained by a relatively greater change in the higher
343 order J_k values.

344 This research proposes a multi-step strategy to implement the calibration of the elastic
345 wave speed and the viscoelastic compliances. The FRD of a viscoelastic pipeline in a
346 reservoir-pipeline-high loss valve system can be extracted by hydraulic transient tests and
347 the resonant frequencies are determined by locating the peaks in the FRD. Without loss of
348 generality, a high loss inline valve is considered, although a fully closed inline valve is
349 preferred. The resonant frequencies are shifted due to unsteady friction and viscoelasticity
350 when compared with those in a theoretical frictionless and elastic pipe. As the calibration
351 of the viscoelastic parameters is the focus, an approach is proposed to correct the shifting
352 of the resonant frequencies induced by the effects of unsteady friction before the ultimate

353 calibration for the viscoelastic parameters. The elastic wave speed and the viscoelastic
354 compliances are firstly estimated from the originally measured resonant frequencies by
355 solving Eq. (15) with neglecting the effects of friction (i.e. $T_F = 1$). Considering that the
356 shifting in resonant frequencies due to the unsteady friction is insignificant, the estimated
357 wave speed should be close to the true elastic wave speed, though the estimated viscoelastic
358 compliances may have significant error. Using this estimated elastic wave speed and the
359 friction factor estimated from the steady state, numerical simulations can be conducted to
360 estimate the resonant frequencies for the scenario elastic and frictionless (EL) and the
361 scenario elastic with unsteady friction (EL+UF). The contribution of the unsteady friction
362 to the shifting of the resonant frequencies can be evaluated from the numerical results, and
363 then corrected from the measured resonant frequencies. The corrected resonant frequencies,
364 with the unsteady friction-induced shifting largely corrected, are then used in Eq. (15) for
365 the calibration of the elastic wave speed and the viscoelastic compliances. The detailed
366 procedure for the systematic evaluation of the elastic wave speed and the viscoelastic
367 compliances is summarized in the following steps:

- 368 1. For a viscoelastic pipeline in a reservoir-pipeline-high loss valve configuration,
369 determine the Darcy-Weisbach friction factor f using the steady-state head loss,
370 and the Reynolds number R from the steady-state flow.
- 371 2. Extract the frequency response diagram (FRD) of the viscoelastic pipeline system.
372 Techniques for FRD extraction in real pipelines can be found in Lee et al. (2006;
373 2008) and Gong et al. (2015a). The resonant frequencies, ω_m , are then read from
374 the measured FRD by locating the peaks of the pressure response.

- 375 3. Solve the set of nonlinear equations defined by Eq. (15) for $m=1, \dots, M$,
376 neglecting the influence of the friction term (i.e. $T_F = 1$) to estimate the elastic
377 wave speed a_e and the viscoelastic compliances J_k . The number of equations M
378 (the number of resonant frequencies used in the parameter calibration) has to be
379 equal or more than the number of unknown parameters. For example, if a three-
380 element K-V model is used and τ_k are fixed to reduce the possibility of non-
381 uniqueness in solutions, as adopted in other studies (Covas et al. 2005; Soares et al.
382 2008; Keramat and Haghghi 2014), there are four unknowns to determine,
383 including a_e , J_1 , J_2 and J_3 . As a result, four or more resonant frequencies in the
384 measured FRD should be used. The values of τ_k used should be significantly
385 different from one another and all smaller than one half the fundamental pipeline
386 period (see the sub-section *Retardation time and pipe period* later in this paper for
387 more discussion).
- 388 4. Calculate the resonant frequencies using Eq. (15) neglecting both the effects of
389 viscoelasticity and friction (i.e. $T_{VE} = 1$ and $T_F = 1$) for a corresponding frictionless
390 and elastic pipeline system. This is achieved by substituting the elastic wave speed
391 a_e determined in Step 3 into Eq. (15). The results, symbolized as ω_{m_FL} , are the
392 estimated resonant frequencies for the corresponding frictionless and elastic
393 pipeline system.
- 394 5. Calculate the resonant frequencies using Eq. (15) neglecting the effects of
395 viscoelasticity (i.e. $T_{VE} = 1$) for a corresponding elastic pipeline system with
396 unsteady friction. This is achieved by substituting the Darcy-Weisbach friction

397 factor f and the Reynolds number R determined in Step 1 and the elastic wave
398 speed a_e determined in Step 3 into Eq. (15). The results, symbolized as ω_{m_UF} , are
399 the estimated resonant frequencies for the corresponding elastic pipeline with
400 unsteady friction.

401 6. Correct the measured resonant frequencies obtained in Step 2 to remove the shifting
402 induced by unsteady friction. The correction is achieved by the formula

403

$$\omega_{m_C} = \omega_m \frac{\omega_{m_FL}}{\omega_{m_UF}} \quad (16)$$

404 where ω_{m_C} represents the corrected resonant frequencies. ω_{m_C} is a good
405 approximation of the resonant frequencies for the corresponding frictionless
406 viscoelastic pipeline.

407 7. Repeat Step 3 to determine a_e and J_k but use the corrected resonant frequencies
408 ω_{m_C} obtained in Step 6.

409 The effectiveness of the proposed procedure is verified by numerical simulations, as
410 presented in the section of *Case Studies*.

411 **Case Studies**

412 Numerical simulations are conducted for an HDPE pipeline bounded by a reservoir and an
413 inline valve to verify the proposed technique for the calibration of the creep function (the
414 elastic wave speed and the viscoelastic compliances). A discharge perturbation [defined in

415 Eq. (11)] is used as the transient excitation, which can be realized by abruptly opening and
416 then closing a side-discharge valve located just upstream of the inline valve. Two case
417 studies are considered: one is a reservoir-pipeline-closed valve system without friction and
418 another is a reservoir-pipeline-high loss valve system with the consideration of unsteady
419 friction.

420 ***System specifications***

421 The physical details of the pipeline system, as given in Table 1, are adapted from the
422 experimental pipeline in the Imperial College as reported in Covas et al. (2004), but the
423 length of the pipe is doubled in the Case Studies to ensure all creep elements fully act
424 within half period of a water hammer cycle so that they are possible to be calibrated (more
425 discussion in the later sub-section *Retardation time and pipe period*). Note that the steady-
426 state flow rate 0.3 L/s is for the reservoir-pipeline-high loss valve configuration (case study
427 2) and it is zero for the configuration where the inline valve is fully closed (case study 1).
428 The elastic wave speed a_e , which is to be calibrated, is 395 m/s and given in Table 1. The
429 viscoelastic parameters are from one of the experimentally calibrated results in Covas et al.
430 (2004), and they are given in Table 2. Research by Covas et al. (2004) showed that the use
431 of three viscoelastic elements in the K-V model is sufficient enough to describe the
432 viscoelasticity of a HDPE pipeline. The compliance coefficients J_1 to J_3 are to be
433 determined by the proposed technique.

434 **Case study 1: reservoir-pipeline-closed valve**

435 The reservoir-pipeline-closed valve configuration is the suggested configuration for the
436 calibration of the pipeline viscoelastic parameters. The effects of friction are small because
437 of the zero steady-state flow and Eq. (13), in which the impedance of the valve is not
438 involved, is the governing equation for the frequency response function of the system. A
439 frictionless pipeline is considered in this case study.

440 **Theoretical frequency response diagrams**

441 Using Eq. (13) and neglecting friction, the theoretical frequency response diagrams (FRDs)
442 for the scenarios: (a) elastic and frictionless (EL) and (b) viscoelastic and frictionless (VE)
443 are obtained and illustrated in Figure 3. For the scenario of EL (solid line in Figure 3), the
444 resonant responses are infinite and therefore cannot be fully shown in the figure. The first
445 four resonant angular frequencies for the two FRDs respectively are read and given in Table
446 3. It can be seen from Figure 3 and Table 3 that the pipe wall viscoelasticity introduces
447 non-uniform shifting of the resonant frequencies and non-uniform reduction of the
448 amplitude of the resonant responses.

449 **Parameter evaluation**

450 The calibration of the elastic wave speed a_e and the viscoelastic parameters J_1 to J_3 is
451 relatively easy when the effect of friction is negligible. The procedure is as described in
452 Steps 1 to 3 in the sub-section *Steps for implementation*. Once the first four resonant
453 frequencies ω_m ($m = 1$ to 4) are determined (as given in Table 3), four nonlinear equations
454 can be established from Eq. (15). Solving the four nonlinear equations gives the elastic

455 wave speed a_e and the viscoelastic parameters J_1 to J_3 and the results are summarized in
 456 Table 4. In this research, the shuffled complex evolution (SCE) algorithm (Duan et al. 1993)
 457 is used to search the values for a_e and J_1 to J_3 by minimizing the objective function

$$F(a_e, J_k) = \sum_{m=1}^M \left[\frac{\omega_m |T_{VE}|}{a_e (2m-1)} - \frac{\pi}{2} \right]^2 \quad (16)$$

458 Note that T_{VE} is given in Eq. (7) and is a function of a_e , J_k and ω_m . The search space is
 459 limited to the range of [350, 450] for a_e and [1E-11, 1E-9] for the J_k , as these are
 460 physically plausible ranges for a HDPE pipe according to the study by Covas et al. (2005).

461 It can be seen from Table 4 that the calibrated results are very close to the theoretical results
 462 used in the original model. The difference is due to the simplifications and approximations
 463 used in the derivation of Eq. (15). The calibrated FRD is compared with the theoretical
 464 FRD for the scenario of viscoelastic and frictionless in Figure 4. The close similarity
 465 between the calibrated and the theoretical FRDs indicates that the calibrated results can
 466 appropriately represent the viscoelastic behavior of the pipeline system. Case study 1
 467 verifies that the proposed technique is valid for a frictionless viscoelastic pipeline.

468 **Case study 2: reservoir-pipeline-high loss valve**

469 The reservoir-pipeline-high loss valve configuration is studied in this case study. Due to
 470 the existence of steady-state flow, the effects of friction are typically not negligible in the

471 calibration of the viscoelastic parameters. Eq. (12) is the governing equation for the
472 frequency response function of the system.

473 **Theoretical frequency response diagrams**

474 The theoretical frequency response diagrams (FRDs) of the reservoir-pipeline-high loss
475 valve system are simulated by Eq. (12) for the scenarios: (a) elastic and frictionless (EL);
476 (b) elastic with steady and unsteady friction (EL+UF); (c) viscoelastic and frictionless (VE);
477 and (d) viscoelastic with steady and unsteady friction (VE +UF), and the results are given
478 in Figure 5. The first four resonant angular frequencies for the four FRDs respectively are
479 read and given in Table 5.

480 It can be seen from Figure 5 and Table 5 that both the unsteady friction and the
481 viscoelasticity shift the resonant frequencies of the pipeline system, although the shifting
482 induced by the unsteady friction is much less than that induced by the viscoelasticity. The
483 scenario of VE +UF experiences the greatest shifting from the theoretical resonant
484 frequencies of the EL case. The numerical results also confirm that both the unsteady
485 friction and the viscoelasticity can introduce non-uniform reduction in the size of the
486 resonant responses.

487 **Parameter evaluation**

488 The elastic wave speed a_e and the viscoelastic compliances J_1 to J_3 are determined using
489 the procedure proposed in the sub-section *Steps for implementation*. In addition to the
490 steady-state hydraulic condition, it is assumed that only the FRD (or the resonant

491 frequencies) of the scenario of VE+UF is known because this is the scenario for a real
492 reservoir-pipeline-high loss valve system.

493 Estimate the elastic wave speed neglecting friction:

494 The elastic wave speed is estimated using the measured resonant frequencies by following
495 the instructions in Steps 1 to 3. Four equations are established using Eq. (15) for $m = 1$ to
496 4. The SEC is used to solve the equations and the results of the calibration using the
497 resonant frequencies from the scenario VE+UF and neglecting the effect of friction are
498 given in Table 6. The result for the elastic wave speed a_e is very close to the value of 395
499 m/s used in the original model. The calibrated J_k have significant discrepancies from the
500 values used in the original model, which indicates that the effects of friction cannot simply
501 be neglected in the calibration process for this case study.

502 Correct the shifting in resonant frequencies induced by unsteady friction:

503 Steps 4 to 6 are conducted to correct the effects of unsteady friction on the shifting of the
504 resonant frequencies. The approximation of the resonant angular frequencies (ω_{m_c}) for
505 the viscoelastic and frictionless (VE) scenario is obtained, and the results are given in Table
506 7. The resonant angular frequencies for the scenarios of EL and EL+UF are calculated
507 using Eq. (15) with the elastic wave speed $a_e = 396.9$ m/s as calibrated in Step 3. The
508 approximation of the resonant angular frequencies (ω_{m_c}) for scenario VE is obtained from
509 Eq. (16). It can be seen that the estimated resonant frequencies is very close to the

510 theoretical results for the scenario VE shown in Table 5 where unsteady friction is not
511 included in the model.

512 Calibration using the corrected resonant frequencies:

513 The final stage for the parameter evaluation is the Step 7 in the proposed procedure. The
514 estimated resonant frequencies for the scenario VE are substituted into Eq. (15) and the
515 SCE algorithm is run to obtain the results, which are presented in Table 8. The results show
516 that the elastic wave speed and the viscoelastic compliances are all calibrated with
517 acceptable accuracy compared with the values used in the original pipeline model. The
518 viscoelastic compliances are much better calibrated when compared with the results in
519 Table 6, where the effects of friction were simply neglected. The significant improvement
520 in accuracy verifies that the proposed approach for correcting the effects of unsteady
521 friction is useful.

522 The FRD for the scenario viscoelastic and frictionless (VE) is simulated using Eq. (12)
523 with the calibrated parameters in Table 8. The results are given in Figure 6 as the dashed
524 line, with the comparison to the theoretical FRD for scenario VE (the solid line) obtained
525 from the values of these parameters in the original model. A generally good match is
526 observed in Figure 6 between the calibrated FRD and the theoretical FRD, which indicates
527 that the calibrated parameters can be used to describe the viscoelastic characteristics of the
528 pipeline system.

529 **Discussions**

530 The outlined numerical case study shows that the proposed technique for the calibration of
531 the creep function of viscoelastic pipelines is effective even when unsteady friction is
532 present. However, a few practical issues that may bring challenges in future field
533 applications are identified and discussed as follows:

534 ***Retardation time and pipe period***

535 The proposed technique calibrates the elastic wave speed and the viscoelastic compliances
536 based on resonant frequencies and a set of preselected retardation times. The numerical
537 *Case Studies* reported in a previous section used a pipe length two times that in the original
538 laboratory pipeline system in Covas et al. (2004). The increase in length was adopted to
539 ensure that the pipe is long enough that all the K-V elements have enough time (within the
540 half period of any water hammer cycle) to significantly respond before a change in the
541 pressure loading. Research in the time domain showed that compliances with a retardation
542 time greater than one half the period are unable to be calibrated with accuracy because the
543 retardation effects from them are not fully expressed before a change in loading (Keramat
544 and Haghghi 2014). In the *Case Studies*, the viscoelastic parameters are kept the same as
545 those in Covas et al. (2004) so that the viscoelastic properties of the pipeline are kept the
546 same. The third retardation time τ_3 is 1.5 s and is greater than one half the period of the
547 water hammer cycle (approximately 1.4 s as estimated by $2L/a_e$) if the original pipe
548 length of 277 m is used. As a result, the pipe length was doubled in the *Case Studies* to
549 make sure all the K-V elements can fully respond within one half the period of the water
550 hammer cycle.

551 Extra numerical simulations are conducted in this research after modifying the length of
552 the pipe to 277 m [the original length of the laboratory system in Covas et al. (2004), half
553 the length considered in the *Case Studies* section]. A reservoir-pipeline-closed valve
554 configuration is considered and the pipeline is assumed as frictionless in the original model.
555 While keeping the viscoelastic compliances (J_1 to J_3) the same as those used in the *Case*
556 *Studies*, two sets of retardation time (τ_1 to τ_3) are used to generate two theoretical FRDs
557 by Eq. (13). The first set are the same as those used in the *Case Studies* and they are $\tau_1 =$
558 0.05 s, $\tau_2 = 0.5$ s and $\tau_3 = 1.5$ s. The second set are $\tau_1 = 0.05$ s, $\tau_2 = 0.25$ s and $\tau_3 = 1.0$
559 s so that the retardation time are significantly different from one another and all are smaller
560 than one half the period of the water hammer cycle (approximately 1.4 s). Two sets of the
561 elastic wave speed and the viscoelastic compliances are then calibrated from the two
562 theoretical FRDs by following the Steps 1 to 3 presented in the sub-section *Steps for*
563 *implementation* (same procedure as used in Case study 1). The results are summarized in
564 Table 9.

565 Comparing the results shown in Table 9 with the results of the previous Case study 1 in
566 Table 4, it can be seen that when the length of the pipe is changed from 554 m (Table 4) to
567 277 m (Table 9) but the viscoelastic parameters are all kept the same, J_2 and J_3 cannot be
568 calibrated with acceptable accuracy because the τ_3 is greater than one half the period of
569 the water hammer cycle. However, when the second set of the retardation times ($\tau_1 = 0.05$
570 s, $\tau_2 = 0.25$ s and $\tau_3 = 1.0$ s) are used in the original model and also in the calibration
571 process, all the viscoelastic compliances are calibrated with high accuracy. Several other

572 sets of retardation times that satisfy the criteria “significantly different from one another
573 and all smaller than one half the period of the water hammer cycle” are also studied and
574 they all yield successful calibration.

575 The numerical simulations confirm that the selection of the set of retardation times is
576 critical for the calibration of viscoelastic compliances. For a real viscoelastic pipeline with
577 a specific length and elastic wave speed, the set of retardation times should be selected as
578 significantly different from one another and all smaller than one half the period of the water
579 hammer cycle. Further analysis on the importance of pipe system scale, in particular pipe
580 length and diameter, on viscoelastic behavior in pipe transients is suggested for future
581 research.

582 ***Influence of the characteristic impedance***

583 In the proposed parameter evaluation technique, it is assumed that the measured resonant
584 frequencies (which are actually the peak frequencies of the function $|Z \tanh(\mu L)|$) are the
585 frequencies where the function $|\tanh(\mu L)|$ reaches its maxima. This inevitably introduces
586 error into the parameter calibration because Z is a frequency-dependent function rather
587 than a constant number. As defined in Eq. (6), the values of Z depend on the viscoelastic
588 and the friction terms, and they are typically unknown or have great uncertainties for real
589 pipeline applications. As a result, the effects from Z on the resonant frequencies are
590 difficult to assess or correct before the parameter calibration.

591 However, the values of Z are calculated numerically for the pipeline system discussed in
592 the *Case Studies*, and its absolute values are plotted in Figure 7. The effects of Z is
593 evaluated for the *Case Studies* by calculating the difference between the peak frequencies
594 of $|Z \tanh(\mu L)|$ and those of $|\tanh(\mu L)|$, both for the VE scenario, and the results are given
595 in Figure 8.

596 It can be seen from Figure 7 that Z is a monotonic function of frequency. From Figure 8,
597 the differences in the peak frequencies between the functions $|Z \tanh(\mu L)|$ and $|\tanh(\mu L)|$
598 are observed to be small. Numerical simulations in Case study 1 showed that the effects of
599 the assumption on the determination of the elastic wave speed and the viscoelastic
600 compliances are small (the maximum relative error induced was less than 4% as shown in
601 Table 4). A more detailed analysis of the influence of Z is recommended for future
602 research.

603 ***Determination of the resonant frequencies***

604 The successful application of the proposed technique relies on the accurate determination
605 of the resonant frequencies of a pipeline system. The determination of the resonant
606 frequencies typically requires the extraction of the frequency response diagram (FRD).
607 Two challenges exist (which also apply to all FRD-based techniques): the bandwidth of the
608 transient excitation and the specific boundary condition required (Lee et al. 2013).
609 Fortunately, the proposed technique for the calibration of the creep function only requires
610 the first few resonant peaks to be measured and viscoelastic pipelines typically has a low
611 fundamental frequency due to low wave speeds. Consider the pipeline used in the *Case*

612 *Studies* as an example (a 557 m HDPE pipe with an elastic wave speed of 395 m/s), the
613 bandwidth of the transient excitation is required to be just higher than 1.2 Hz, which is easy
614 to achieve even by a manual valve closure. The specific boundary condition required for
615 the proposed technique is a reservoir-pipeline-valve (RPV) configuration. This is typically
616 not readily available in complex pipeline networks. Lee et al. (2005) proposed a technique
617 to subdivide complex systems into individual single pipes for the purpose of FRD
618 extraction by using a close in-line valve and a junction as the boundaries. The side-
619 discharge valve-based transient generator recently developed by the authors (Gong et al.
620 2015a) can be useful in extracting the FRD of a viscoelastic pipeline by using persistent
621 pseudo random binary signals. However, experimental verification is needed in the future.

622 ***Effects of complexities in real pipelines***

623 In addition to frictional effects, real pipelines may have complexities such as faults and
624 significant fluid structure interaction (FSI). Studies on elastic pipelines show that the
625 influence of discrete faults, including leaks and discrete blockage, on the resonant
626 frequencies of a pipeline system is negligible (Lee et al. 2005). However, extended wall
627 deterioration, such as extended blockages, can slightly alter the resonant frequencies (Lee
628 et al. 2013). FSI, in particular the axial oscillation of the pipeline during transient events,
629 may also have some impact on the resonant frequencies (Keramat et al. 2012), but the
630 details are yet to be explored in the future.

631 **Conclusions**

632 A new technique has been proposed for calibrating the elastic wave speed and the
633 viscoelastic compliances in viscoelastic pipelines using hydraulic transient analysis, which
634 is the first viscoelastic parameter estimation technique developed in the frequency domain.
635 The transfer matrix of a viscoelastic pipeline, with steady and unsteady friction considered,
636 has been derived from the time-domain one-dimensional continuity and momentum water
637 hammer equations, where an extra viscoelastic term is included in the continuity equation
638 to represent the retarded strain. A generalized Kelvin-Voigt (K-V) model with multiple
639 viscoelastic elements is used to describe the creep function. It has been found that the use
640 of a viscoelastic term in the continuity equation in the time-domain is equivalent to the use
641 of a frequency-dependent complex wave speed (or modulus of elasticity) in the frequency-
642 domain. The frequency response function (FRF) of a viscoelastic pipeline in a reservoir-
643 pipeline-high loss valve configuration has been derived, from which the relationship
644 between the resonant frequencies and the pipeline elastic wave speed and viscoelastic
645 compliances are analytically established. A parameter calibration technique has been
646 proposed for the evaluation of these parameters using the resonant frequencies. Detailed
647 steps for implementing the technique have been presented, including an approach for
648 correcting the shifting in resonant frequencies induced by unsteady friction. The parameter
649 evaluation is achieved by solving a set of nonlinear equations, which is much more
650 computational efficient (less than 2 s in this study for solving four equations using the
651 shuffled complex evolution algorithm) than the conventional inverse transient analysis
652 (ITA)-based parameter calibration. For the first time, the elastic wave speed is calibrated
653 together with the viscoelastic compliance in the frequency domain, rather than being

654 estimated separately in the time domain. The proposed technique only uses information
655 about the resonant frequencies, which is not subject to discrete faults (such as leaks) in
656 pipelines.

657 Numerical case studies have been conducted on an HDPE pipeline to verify the proposed
658 technique. A three K-V element model has been used to simulate the pipeline viscoelastic
659 effects. For a frictionless pipeline (case study 1), the elastic wave speed and viscoelastic
660 compliances are calibrated with high accuracy (less than 4 % relative error compared with
661 the theoretical values used in the original pipeline model). When unsteady friction is
662 considered (case study 2), the approach correcting the unsteady friction-induced shifting
663 of the resonant frequencies is proved to be useful and significantly improves the accuracy
664 of the calibration. It is also worth noting that the elastic wave speed can be calibrated with
665 a high accuracy (less than 1% relative error compared with the theoretical value) no matter
666 whether the effect of unsteady friction is corrected or not. Practical issues that may bring
667 challenges in future field applications, including the selection of the retardation times, the
668 influence of the characteristic impedance, the determination of the resonant frequencies
669 and some complexities in real pipeline systems, have been discussed in the section
670 *Discussions* in the paper.

671 Overall, the proposed frequency-domain technique is a step forward towards accurate
672 calibration of the creep function of viscoelastic pipelines. The elastic wave speed and the
673 viscoelastic compliances can be calibrated with satisfactory accuracy provided that a few
674 resonant frequencies of a viscoelastic pipeline system are known.

675 **Acknowledgements**

676 The research presented in this paper has been supported by the Australia Research Council
677 through the Discovery Project Grant DP140100994.

678 **Notation**

679 *The following symbols are used in this paper:*

- A = pipe cross sectional area (m^2);
- a_c = frequency-dependent complex wave speed derived from the use
of retarded strain term (-);
- a_e = elastic wave speed (m/s);
- a^* = frequency-dependent complex wave speed derived from
complex modulus of elasticity (-);
- D = internal pipe diameter (m);
- E_0 = elastic modulus of elasticity (Pa);
- E_k = modulus of elasticity for the k th viscoelastic element (Pa);
- e = wall thickness of a pipe (m);
- $F()$ = objective function (-);
- f = Darcy-Weisbach friction factor (-);
- g = gravitational acceleration (ms^{-2});
- H = piezometric head (m);
- H_0 = steady-state head (m);
- h = complex head oscillation (m);

- h_f = head loss per unit length due to friction (m);
 h^* = normalized complex head oscillation (m^2s);
 i = imaginary unit (-);
 $J(\)$ = creep (compliance) function (Pa^{-1});
 J_0 = elastic compliance, E_0^{-1} (Pa^{-1});
 J_k = viscoelastic compliance, E_k^{-1} (Pa^{-1});
 L = length of pipe (m);
 M = total number of resonant frequencies used (-);
 N = total number of viscoelastic elements used (-);
 Q = flow rate (m^3s^{-1});
 q = complex flow oscillation (m^3s^{-1});
 R = resistance coefficient (sm^{-3});
 R_s = resistance from steady friction (sm^{-3});
 R_{us} = resistance from unsteady friction (sm^{-3});
 \mathbf{R} = Reynolds number (-);
 T_F = friction term in the characteristic impedance and propagation operator (-);
 T_{VE} = viscoelastic term in the characteristic impedance and propagation operator (-);
 t = time (s);
 x = spatial coordinate (m);
 Z = characteristic impedance (m^2s);

680

681 *Greek symbols:*

- Δq = discharge perturbation (m^3/s);
- α = pipeline restraint factor (-);
- ε_r = total retarded strain (-);
- η_k = viscosity for the k th viscoelastic element;
- μ = propagation operator (m^{-1});
- ρ = fluid density (kgm^{-3});
- τ_k = retardation time for the k th viscoelastic element (s);
- ω = angular frequency (rad);
- ω_m = resonant angular frequency (rad);
- ω_{m_C} = approximation of the resonant angular frequency for a frictionless viscoelastic pipeline (rad);
- ω_{m_EL} = calculated resonant angular frequency for a frictionless elastic pipeline (rad);
- ω_{m_UF} = calculated resonant angular frequency for an elastic pipeline with steady and unsteady friction (rad);

682

683 **References**

- 684 Brunone, B., Golia, U. M., and Greco, M. (1995). "Effects of two-dimensionality on pipe
685 transients modeling." *Journal of Hydraulic Engineering*, 121(12), 906-912.
- 686 Brunone, B., Karney, B. W., Mecarelli, M., and Ferrante, M. (2000). "Velocity profiles
687 and unsteady pipe friction in transient flow." *Journal of Water Resources
688 Planning and Management*, 126(4), 236-244.

689 Brunone, B., and Berni, A. (2010). "Wall Shear Stress in Transient Turbulent Pipe Flow
690 by Local Velocity Measurement." *Journal of Hydraulic Engineering*, 136(10),
691 716-726.

692 Chaudhry, M. H. (2014). *Applied Hydraulic Transients*, 3rd Ed., Springer, New York,
693 NY.

694 Covas, D., Stoianov, I., Mano, J. F., Ramos, H., Graham, N., and Maksimovic, C. (2004).
695 "The dynamic effect of pipe-wall viscoelasticity in hydraulic transients. Part I -
696 Experimental analysis and creep characterization." *Journal of Hydraulic
697 Research*, 42(5), 516-530.

698 Covas, D., Stoianov, I., Mano, J. F., Ramos, H., Graham, N., and Maksimovic, C. (2005).
699 "The dynamic effect of pipe-wall viscoelasticity in hydraulic transients. Part II -
700 Model development, calibration and verification." *Journal of Hydraulic Research*,
701 43(1), 56-70.

702 Duan, H.-F., Ghidaoui, M., Lee, P. J., and Tung, Y.-K. (2010a). "Unsteady friction and
703 visco-elasticity in pipe fluid transients." *Journal of Hydraulic Research*, 48(3),
704 354-362.

705 Duan, H.-F., Ghidaoui, M. S., and Tung, Y.-K. (2010b). "Energy analysis of
706 viscoelasticity effect in pipe fluid transients." *Journal of Applied Mechanics,
707 Transactions ASME*, 77(4), 1-5.

708 Duan, H.-F., Lee, P. J., Ghidaoui, M. S., and Tung, Y.-K. (2012). "System response
709 function-based leak detection in viscoelastic pipelines." *Journal of Hydraulic
710 Engineering*, 138(2), 143-153.

711 Duan, Q. Y., Gupta, V. K., and Sorooshian, S. (1993). "Shuffled complex evolution
712 approach for effective and efficient global minimization." *Journal of Optimization
713 Theory and Applications*, 76(3), 501-521.

714 Ferrante, M., Massari, C., Brunone, B., and Meniconi, S. (2013). "Leak behaviour in
715 pressurized PVC pipes." *Water Science and Technology: Water Supply*, 13(4),
716 987-992.

717 Franke, P. G., and Seyler, F. (1983). "Computation of unsteady pipe flow with respect to
718 visco-elastic material." *Journal of Hydraulic Research*, 21(5), 345-353.

719 Gally, M., Güney, M., and Rieutord, E. (1979). "An Investigation of Pressure Transients
720 in Viscoelastic Pipes." *Journal of Fluids Engineering*, 101(4), 495-499.

721 Gong, J., Lambert, M. F., Simpson, A. R., and Zecchin, A. C. (2013). "Single-event leak
722 detection in pipeline using first three resonant responses." *Journal of Hydraulic
723 Engineering*, 139(6), 645-655.

724 Gong, J., Lambert, M. F., Zecchin, A. C., and Simpson, A. R. (2015a). "Experimental
725 verification of pipeline frequency response extraction and leak detection using the
726 inverse repeat signal." *Journal of Hydraulic Research*, published online on 11
727 December 2015, DOI: 10.1080/00221686.2015.1116115.

728 Gong, J., Zecchin, A. C., Lambert, M. F., and Simpson, A. R. (2015b). "Study on the
729 frequency response function of viscoelastic pipelines using a multi-element
730 Kevin-Voigt model." *Procedia Engineering*, 119, 226-234.

731 Güney, M. S. (1983). "Waterhammer in viscoelastic pipes where cross-section parameters
732 are time dependent." *BHRA Fluid Engineering*, 189-204.

733 Keramat, A., Tijsseling, A. S., and Ahmadi, A. (2010). "Investigation of transient
734 cavitating flow in viscoelastic pipes." Institute of Physics Publishing.

735 Keramat, A., Tijsseling, A. S., Hou, Q., and Ahmadi, A. (2012). "Fluid-structure
736 interaction with pipe-wall viscoelasticity during water hammer." *Journal of Fluids
737 and Structures*, 28, 434-455.

738 Keramat, A., Kolahi, A. G., and Ahmadi, A. (2013). "Waterhammer modelling of
739 viscoelastic pipes with a time-dependent Poisson's ratio." *Journal of Fluids and
740 Structures*, 43, 164-178.

741 Keramat, A., and Haghghi, A. (2014). "Straightforward transient-based approach for the
742 creep function determination in viscoelastic pipes." *Journal of Hydraulic
743 Engineering*, 140(12), 04014058.

744 Kreyszig, E., Kreyszig, H., and Norminton, E. J. (2011). *Advanced Engineering
745 Mathematics*, 10th Ed., John Wylie & Sons, Inc, Hoboken, N.J.

746 Lazhar, A., Hadj-Taieb, L., and Hadj-Taieb, E. (2013). "Two leaks detection in
747 viscoelastic pipeline systems by means of transient." *Journal of Loss Prevention
748 in the Process Industries*, 26(6), 1341-1351.

749 Lee, P. J., Vítkovský, J. P., Lambert, M. F., Simpson, A. R., and Liggett, J. A. (2005).
750 "Frequency domain analysis for detecting pipeline leaks." *Journal of Hydraulic
751 Engineering*, 131(7), 596-604.

752 Lee, P. J., Lambert, M. F., Simpson, A. R., Vítkovský, J. P., and Liggett, J. A. (2006).
753 "Experimental verification of the frequency response method for pipeline leak
754 detection." *Journal of Hydraulic Research*, 44(5), 693-707.

755 Lee, P. J., Vítkovský, J. P., Lambert, M. F., and Simpson, A. R. (2008). "Valve design for
756 extracting response functions from hydraulic systems using pseudorandom binary
757 signals." *Journal of Hydraulic Engineering*, 136(4), 858-864.

758 Lee, P. J., Duan, H. F., Ghidaoui, M., and Karney, B. (2013). "Frequency domain
759 analysis of pipe fluid transient behaviour." *Journal of Hydraulic Research*, 51(6),
760 609-622.

761 Liggett, J. A., and Chen, L.-C. (1994). "Inverse transient analysis in pipe networks."
762 *Journal of Hydraulic Engineering*, 120(8), 934-955.

763 Meißner, E., and Frank, G. (1977). "Influence of pipe material on the dampening of water
764 hammer." *Proceedings of the 17th Congress of the International Association for
765 Hydraulic Research*, IAHR, Baden-Baden, Gemany.

766 Meniconi, S., Brunone, B., Ferrante, M., and Massari, C. (2012). "Transient
767 hydrodynamics of in-line valves in viscoelastic pressurized pipes: Long-period
768 analysis." *Experiments in Fluids*, 53(1), 265-275.

769 Meniconi, S., Duan, H. F., Lee, P. J., Brunone, B., Ghidaoui, M. S., and Ferrante, M.
770 (2013). "Experimental investigation of coupled frequency and time-domain
771 transient test-based techniques for partial blockage detection in pipelines."
772 *Journal of Hydraulic Engineering*, 139(10), 1033-1044.

773 Meniconi, S., Brunone, B., Ferrante, M., and Massari, C. (2014). "Energy dissipation and
774 pressure decay during transients in viscoelastic pipes with an in-line valve."
775 *Journal of Fluids and Structures*, 45, 235-249.

776 Pezzinga, G., and Scandura, P. (1995). "Unsteady flow in installations with polymeric
777 additional pipe." *Journal of Hydraulic Engineering*, 121(11), 802-811.

778 Pezzinga, G., Brunone, B., Cannizzaro, D., Ferrante, M., Meniconi, S., and Berni, A.
779 (2014). "Two-Dimensional Features of Viscoelastic Models of Pipe Transients."
780 *Journal of Hydraulic Engineering*, 140(8), 04014036.

781 Pezzinga, G. (2014). "Evaluation of time evolution of mechanical parameters of
782 polymeric pipes by unsteady flow runs." *Journal of Hydraulic Engineering*,
783 140(12), 04014057.

784 Ramos, H., Covas, D., Borga, A., and Loureiro, D. (2004). "Surge damping analysis in
785 pipe systems: modelling and experiments." *Journal of Hydraulic Research*, 42(4),
786 413-425.

787 Rieutord, E., and Blanchard, A. (1979). "Pulsating viscoelastic pipe flow - water hammer
788 (Ecoulement non permanent en conduite viscoelastique - coup de belier)." *Journal*
789 *of Hydraulic Research*, 17(3), 217-229.

790 Rieutord, E. (1982). "Transient response of fluid viscoelastic lines." *Journal of Fluids*
791 *Engineering*, 104(3), 335-341.

792 Sattar, A. M., and Chaudhry, M. H. (2008). "Leak detection in pipelines by frequency
793 response method." *Journal of Hydraulic Research*, 46(sup 1), 138-151.

794 Shaw, M. T., and MacKnight, W. J. (2005). *Introduction to Polymer Viscoelasticity*, 3rd
795 Ed., John Wiley & Sons, Inc, Hoboken, NJ.

796 Soares, A. K., Covas, D. I. C., and Reis, L. F. R. (2008). "Analysis of PVC pipe-wall
797 viscoelasticity during water hammer." *Journal of Hydraulic Engineering*, 134(9),
798 1389-1394.

799 Suo, L., and Wylie, E. B. (1990). "Complex wavespeed and hydraulic transients in
800 viscoelastic pipes." *Journal of Fluids Engineering*, 112(4), 496-500.

801 Vardy, A. E., Kuo-Lun, H., and Brown, J. M. B. (1993). "Weighting function model of
802 transient turbulent pipe friction." *Journal of Hydraulic Research*, 31(4), 533-544.

803 Vardy, A. E., and Brown, J. M. B. (1995). "Transient, turbulent, smooth pipe friction."
804 *Journal of Hydraulic Research*, 33(4), 435-456.

805 Vardy, A. E., and Brown, J. M. (1996). "On turbulent, unsteady, smooth pipe friction."
806 *Proceedings of the 7th International Conference on Pressure Surges and Fluid*
807 *Transients in Pipelines and Open Channels*, Mechanical Engineering
808 Publications, London, UK, 289-311.

809 Vítkovský, J. P., Bergant, A., Simpson, A. R., and Lambert, M. F. (2003). "Frequency-
810 domain transient pipe flow solution including unsteady friction." *Pumps,*
811 *Electromechanical Devices and Systems Applied to Urban Water Management:*
812 *Proceedings of the International Conference*, A. A. Balkema Publishers, Lisse,
813 The Netherlands, 773-780.

814 Vítkovský, J. P., Bergant, A., Simpson, A.R., and Lambert, M.F. (2006). "Systematic
815 Evaluation of One-Dimensional Unsteady Friction Models in Simple Pipelines."
816 *Journal of Hydraulic Engineering*, 132(7), 709-721.

817 Weinerowska-Bords, K. (2006). "Viscoelastic model of waterhammer in single pipeline
818 problems and questions." *Archives of Hydroengineering and Environmental*
819 *Mechanics*, 53(4), 331-351.

820 Weinerowska-Bords, K. (2007). "Accuracy and parameter estimation of elastic and
821 viscoelastic models of the water hammer." *TASK Quarterly : scientific bulletin of*
822 *Academic Computer Centre in Gdansk*, Vol. 11, No 4, 383-395.

823 Wylie, E. B., and Streeter, V. L. (1993). *Fluid Transients in Systems*, Prentice Hall Inc.,
824 Englewood Cliffs, New Jersey, USA.

825 Zecchin, A., Lambert, M., and Simpson, A. (2012). "Inverse laplace transform for
826 transient-state fluid line network simulation." *Journal of Engineering Mechanics*,
827 138(1), 101-115.

828 Zecchin, A. C., Simpson, A. R., and Lambert, M. F. (2008). "von Neumann stability
829 analysis of a method of characteristics visco-elastic pipeline model." *Proceedings*
830 *of the 10th International Conference on Pressure Surges*, BHR Group, Cranfield,
831 UK, 333-347.

832 Zhang, C., and Moore, I. D. (1997). "Nonlinear mechanical response of high density
833 polyethylene. Part I: experimental investigation and model evaluation." *Polymer*
834 *Engineering and Science*, 37(2), 404-413.

835 Zielke, W. (1968). "Frequency-dependent friction in transient pipe flow." *Journal of*
836 *Basic Engineering*, 90(1), 109-115.
837

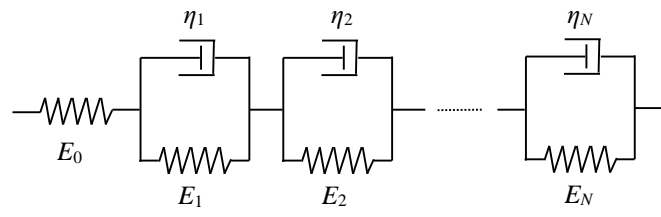


Figure 1. Generalized Kelvin-Voigt model for a viscoelastic solid.

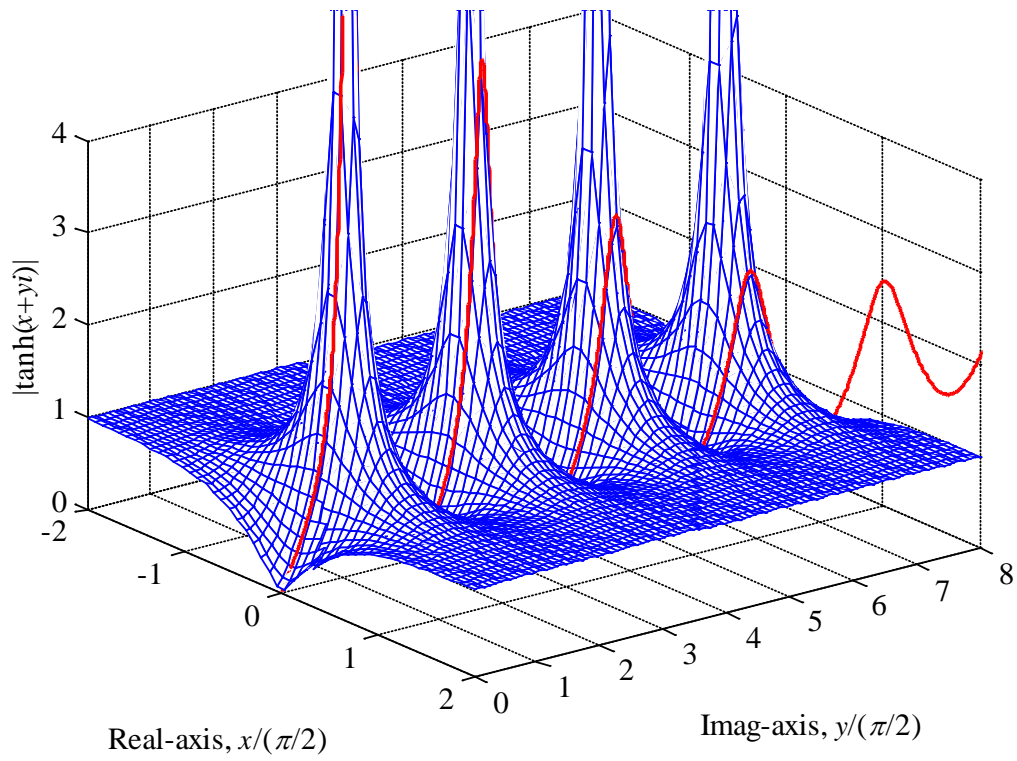


Figure 2. Results of the absolute value of hyperbolic tangent function (the mesh) and a realization of the function $|\tanh(\mu L)|$ (the thick line) for the practical HDPE pipeline considered in the *Case Studies*.

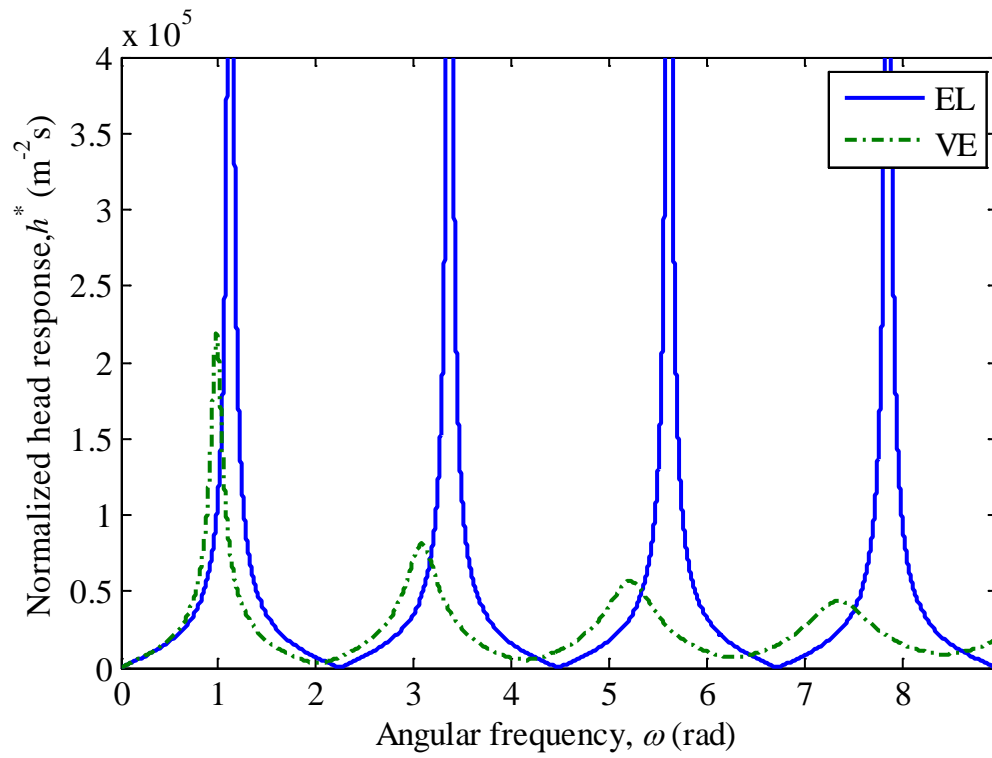


Figure 3. Theoretical FRDs of the reservoir-pipeline-closed valve system (case study 1) for the scenarios: (a) elastic and frictionless (EL, solid line) and (b) viscoelastic and frictionless (VE, dash-dotted line).

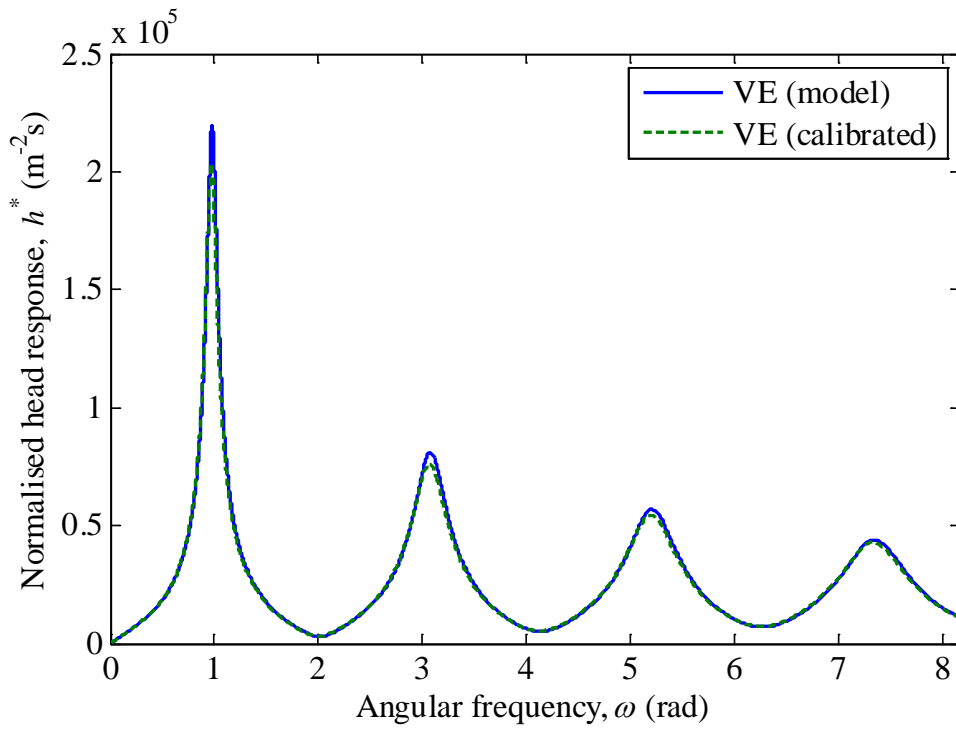


Figure 4. Comparison between the theoretical FRD (the solid line) and the calibrated FRD (the dashed line, using parameters calibrated in case study 1) for scenario VE of a reservoir-pipeline-closed valve system.

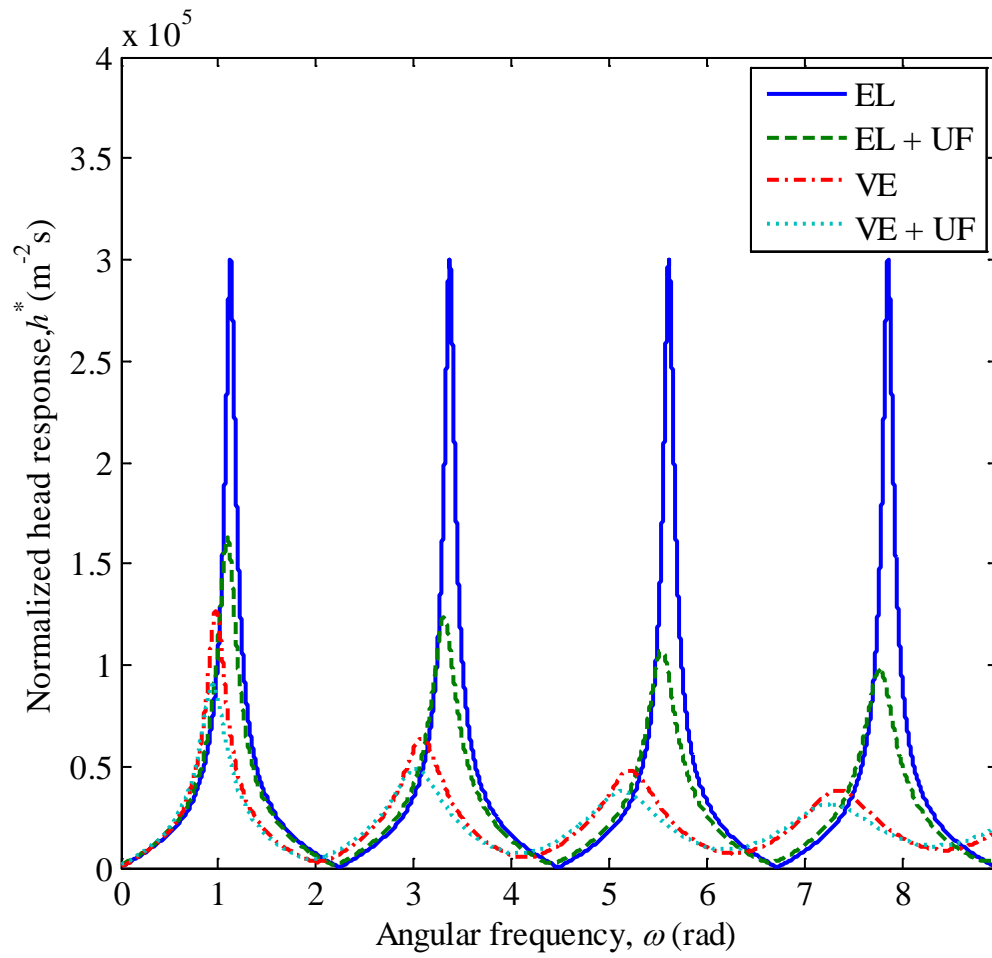


Figure 5. Theoretical FRDs for the scenarios: (a) elastic and frictionless (EL, solid line); (b) elastic with steady and unsteady friction (EL+UF, dashed line); (c) viscoelastic and frictionless (VE, dash-dotted line); and (d) viscoelastic with steady and unsteady friction (VE +UF, dotted line).

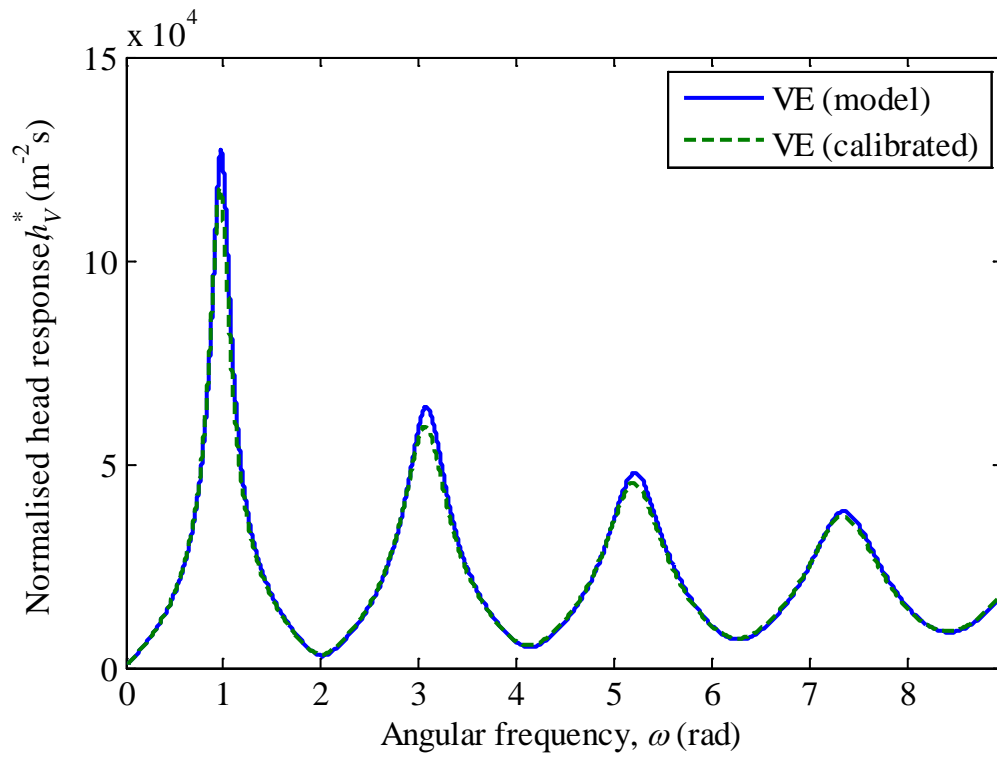


Figure 6. Comparison between the theoretical FRD (the solid line) and the calibrated FRD (the dashed line, use parameters calibrated in case study 2) for scenario VE of a reservoir-pipeline-high loss valve system.

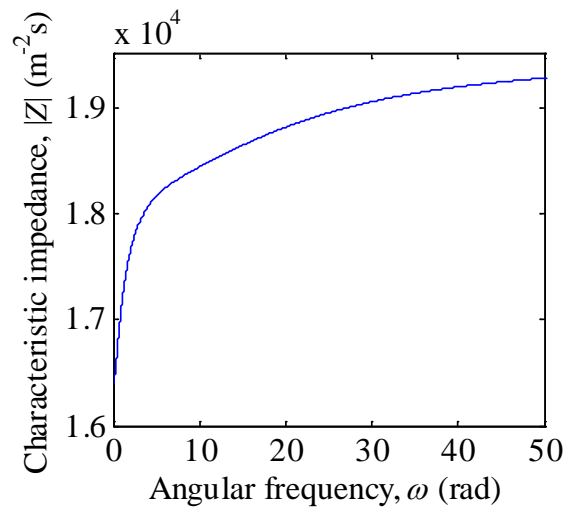


Figure 7. Absolute value of the characteristic impedance for the pipeline system in the *Case Studies*.

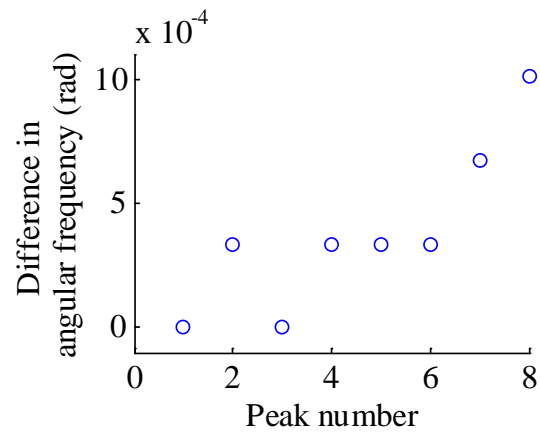


Figure 8. Difference in the peak frequencies between the functions $|Z \tanh(\mu L)|$ and $|\tanh(\mu L)|$ for the scenario viscoelastic and frictionless (VE) in the *Case Studies*.

Tables

Table 1. Specifications of the pipeline system used in the case studies

Parameter	Value
Length L (m)	554
Inner diameter D (mm)	50.6
Wall thickness e (mm)	6.3
Kinematic viscosity ν (m ² /s)	1.004E-6
Fluid density ρ (kg/m ³)	998.2
Head of reservoir (m)	45
Steady-state flow rate (L/s)	0.3
Restraint coefficient α	1.07
Darcy-Weisbach friction factor f	0.02
Reynolds number \mathbf{R}	7519
Elastic wave speed a_e (m/s)	395

Table 2. Viscoelastic parameters used in the case studies

Retardation time τ_k (s)	Compliance J_k (10E-10 Pa ⁻¹)
$\tau_1 = 0.05$	$J_1 = 1.044$
$\tau_2 = 0.5$	$J_2 = 1.037$
$\tau_3 = 1.5$	$J_3 = 1.145$

Table 3. Theoretical resonant angular frequencies for the reservoir-pipeline-closed valve system under the scenarios: (a) elastic and frictionless (EL) and (b) viscoelastic and frictionless (VE).

Peak number m	Theoretical resonant frequency (rad)	
	EL	VE (ω_m)
1	1.120	0.978
2	3.360	3.078
3	5.600	5.208
4	7.840	7.347

Table 4. Results of parameter evaluation using the resonant frequencies from the scenario viscoelastic and frictionless (VE) for *Case study 1*

Parameter	Original model	Calibrated from VE	Relative error
a_e (m/s)	395	394.1	-0.23%
J_1 (10E-10 Pa ⁻¹)	1.044	1.025	-1.78%
J_2 (10E-10 Pa ⁻¹)	1.037	1.070	3.14%
J_3 (10E-10 Pa ⁻¹)	1.145	1.191	3.98%

*Relative error = (Calibrated – Original)/ Original × 100%

Table 5. Theoretical resonant angular frequencies for the reservoir-pipeline-high loss valve system under the scenarios: (a) elastic and frictionless (EL); (b) elastic with steady and unsteady friction (EL+UF); (c) viscoelastic and frictionless (VE); and (d) viscoelastic with steady and unsteady friction (VE +UF).

Peak number <i>m</i>	Theoretical resonant frequency (rad)			
	EL	EL+UF	VE	VE+UF (ω_m)
1	1.120	1.088	0.974	0.943
2	3.360	3.303	3.075	3.019
3	5.600	5.528	5.205	5.135
4	7.840	7.757	7.345	7.264

Table 6. Results of parameter evaluation using the resonant frequencies from the scenario viscoelastic with steady and unsteady friction (VE+UF) neglecting the effects of friction, for

Case study 2.

Parameter	Original model	Calibrated from VE+UF	Relative error
a_e (m/s)	395	396.9	0.49%
J_1 (10E-10 Pa ⁻¹)	1.044	1.314	25.83%
J_2 (10E-10 Pa ⁻¹)	1.037	1.473	42.05%
J_3 (10E-10 Pa ⁻¹)	1.145	1.736	51.64%

*Relative error = (Calibrated – Original)/ Original × 100%

Table 7. Resonant angular frequencies calculated based on the elastic wave speed calibrated in the first attempt for the scenarios: (a) elastic and frictionless (EL); (b) elastic with steady and unsteady friction (EL+UF), and the estimated resonant angular frequencies for the scenario of viscoelastic and frictionless (VE).

Peak number <i>m</i>	Calculated resonant frequency (rad)		
	EL (ω_{m_FL})	EL+UF (ω_{m_UF})	VE approx. (ω_{m_C})
1	1.125	1.093	0.971
2	3.376	3.318	3.072
3	5.627	5.554	5.203
4	7.878	7.794	7.342

Table 8. Results of parameter evaluation using the resonant frequency approximations for scenario viscoelastic and frictionless (VE), for *Case study 2*.

Parameter	Original model	Calibrated from VE approx.	Relative error
a_e (m/s)	395	393.1	-0.49%
J_1 (10E-10 Pa ⁻¹)	1.044	0.983	-5.88%
J_2 (10E-10 Pa ⁻¹)	1.037	1.158	11.64%
J_3 (10E-10 Pa ⁻¹)	1.145	1.373	19.89%

*Relative error = (Calibrated – Original)/ Original × 100%

Table 9. Results of parameter evaluation for the modified pipeline system with a length of 277 m (half of that used in the previous *Case Studies*)

Parameter	Original model	Calibrated with $\tau_1 = 0.05$ s, $\tau_2 = 0.5$ s, $\tau_3 = 1.5$ s	Relative error	Calibrated with $\tau_1 = 0.05$ s, $\tau_2 = 0.25$ s, $\tau_3 = 1.0$ s	Relative error
a_e (m/s)	395	395.1	0.03%	395.3	0.07%
J_1 (10E-10 Pa ⁻¹)	1.044	1.086	3.98%	1.097	5.07%
J_2 (10E-10 Pa ⁻¹)	1.037	7.261	-29.98%	1.043	0.62%
J_3 (10E-10 Pa ⁻¹)	1.145	2.598	126.88%	1.190	3.92%

*Relative error = (Calibrated – Original)/ Original \times 100%